UV-visible emission as a probe of core excitations applied to the furan and carbon dioxide molecules

View the article online for updates and enhancements.

You may also like

- The propagation of low-frequency edge excitations in a two-dimensional electron gas in the IQHE regime
  V I Talyanskii, D R Mace, M Y Simmons et al.

- Hadron resonances as rovibrational states
  Douglas L. Bernardo, Cristiano C. Bastos and Antonio C. Pavão

- Fermions in bosonic string theories
  Justin R. David, Shiraz Minwalla and Carlos Núñez

Recent citations

- O 1s excitation and ionization processes in the CO_2 molecule studied via detection of low-energy fluorescence emission
  A Kivimäki *et al*

UV-visible emission as a probe of core excitations applied to the furan and carbon dioxide molecules

A Kivimäki[1], **M Coreno**[1,2], **J Álvarez Ruiz**[3], **M de Simone**[1], **M Dampc**[4] **and M Zubek**[4]

[1] CNR-INFM, Laboratorio Nazionale TASC, 34149 Trieste, Italy

[2] CNR-IMIP, Monterotondo, 00016 Roma, Italy

[3] Departamento de Química Láser, Instituto de Química-Física Rocasolano Consejo Superior de Investigaciones Científicas, Serrano 119, 28006 Madrid, Spain

[4] Department of Physics of Electronic Phenomena, Gdańsk University of Technology, Narutowicza 11/12, 80233 Gdańsk, Poland

E-mail: `kivimaki@tasc.infm.it`

Abstract. The core excitations of the furan and carbon dioxide molecules have been studied using dispersed UV-visible fluorescence spectroscopy. Balmer-α (Balmer-β) emission was measured at the O 1s and C 1s (O 1s) excitations of furan, while emission due to an excited state of the neutral oxygen atom was measured at the O 1s excitations of CO_2. The excitation functions of the emission lines display both valence and Rydberg resonances, but the latter are more enhanced.

1. Introduction

Fluorescence emission in the ultraviolet and visible regions is commonly observed following core excitations in small molecules, but it is typically the last step in the de-excitation pathway of core-excited and core-ionized states. At first glance, UV-visible fluorescence spectroscopy does not therefore appear particularly suitable for studies of core level processes. Nevertheless, this technique has been exploited in quite a few core-level studies during the last decade or so. The most popular molecular target has been without doubt N_2, and in particular its N 1s $\rightarrow \pi^*$ resonance ([1] and references therein). The (N 1s)$^{-1}\pi^*$ state can decay via participator and spectator resonant Auger transitions to such excited states of the N_2^+ ion that fluoresce directly. Most lines in the UV-visible fluorescence spectrum measured at the N 1s $\rightarrow \pi^*$ excitation of N_2, however, result from excited neutral and ionic fragments (N and N^+) [2] that are created when the final states of resonant Auger decay dissociate. Emission from molecular fragments has also been detected in some molecules. For instance, Chen *et al* [3] determined the excitation function of the CH (A-X) emission at the Cl 2p and Si 2p core edges of $Si(CH_3)_2Cl_2$. Balmer emission due to excited hydrogen atoms has recently showed some promise of being a selective probe of core excitations. The intensity of Balmer-α emission (H(n=3) $\rightarrow$ H(n=2) transition) was found to resonate at the Cl(2p)-to-Rydberg excitations of the HCl molecule, but it was much weaker at the excitations to the empty valence orbitals [4]. Melero García *et al* [5] demonstrated for the O 1s excitations of the H_2O molecule that the different members of the Balmer series are enhanced at different core excitations, the higher members getting most intensity close to the

core ionization potential (IP) where the initial excitations of the O 1s electrons are to high n Rydberg orbitals. Kivimäki *et al* [6] found that Lyman and Balmer emissions are also enhanced at double excitations located above the O 1s edge of the water molecule. It was concluded that whenever core hole states are created with electrons excited to Rydberg orbitals, their signature can be transferred via Auger decay and dissociation to excited hydrogen atoms. Fluorescence emission can, in general, be used to identify excited fragments. However, core hole decay and subsequent dissociation are so complicated processes that all the pathways leading to the creation of a given excited fragment can not be tracked even in diatomic molecules.

In the present investigation, we have measured Balmer emission at the core excitations of the furan molecule. Furan, C_4H_4O, is a heterocyclic aromatic molecule in which the four carbon atoms and one oxygen atom form a planar ring, and one hydrogen atom is bonded to each C atom. Thus furan is the biggest molecule at whose core excitations emission from excited H atoms has been presented. It is also interesting to study whether Balmer emission somehow depends on from which core level (C 1s or O 1s) the excitation starts. In the second part of this paper, we have measured fluorescence emission due to an excited state of the oxygen atom at the O 1s excitations of the CO_2 molecule. This measurement thus presents a case where emission from an atom other than H is used as a probe of core excitations.

2. Experimental

The measurements were performed at the Gas Phase Photoemission beamline [7] of the Elettra synchrotron radiation laboratory (Trieste, Italy). The beamline receives radiation from an undulator in the photon energy range from 13 eV to above 1 keV. Synchrotron radiation was monochomatized by a spherical grating monochromator, equipped with a planar premirror, and sent to the experimental station, where the photon beam crossed a molecular jet emanating from a hypodermic needle. The ambient gas pressure was in the range of 10^{-5} mbar during the experiments. The light emitted in the source region was collimated by a spherical mirror, allowed to exit from the vacuum chamber through a window and focused with a lens onto the entrance slit of the 0.5-m Minuteman 305MV fluorescence spectrograph. Fluorescence light was dispersed with a 1200 lines/mm grating and detected with a liquid-nitrogen cooled CCD detector (Princeton 10:100B). The dispersed fluorescence spectra were recorded at small energy intervals by scanning the photon energy from below the first core excitation feature to above the corresponding ionization limit. At each energy, fluorescence was collected typically for five minutes. The intensity of the emission line of interest was obtained by integrating the counts over the peak and by normalizing to the photon flux of synchrotron radiation measured with a photodiode. A given emission line was always detected on the same part of the CCD detector, hence no sensitivity correction is needed for its relative intensity as a function of photon energy. Total ion yield (TIY) was measured simultaneously with the fluorescence spectra using a microsphere plate. Statistical errors in the TIY and excitation functions are of the order of scattering of adjacent data points at energies where there are no narrow spectral features (for instance, around 550 eV in figure 1).

3. Results and discussion

3.1. Furan

Our TIY of furan measured at the O 1s edge (figure 1) shows the same features (A-C) below the O 1s threshold as was observed in the electron energy loss spectrum (EELS) of Duflot *et al* [8]. Based on *ab initio* calculations, the authors assigned the feature A to the O 1s → 1π* (3b$_1$) transition, the feature B to Rydberg excitations and the feature C to the σ* (C-O) and σ* (C-C) resonances that overlap much weaker Rydberg excitations. Since the TIY was measurered to identify the absorption structures and to compare their intensities with those in the excitation functions, we briefly comment the differences between it and the EELS spectrum of Ref. [8].

The feature D appears in both of them – it was assigned to the σ^* (C-C) resonance in [8] – but the intensity ratio D:C is close to one in figure 1, whereas it is about 1:2 in the EELS. Note that the resonance D is an example of a so-called shape resonance, which can be understood as an excitation to an empty molecular orbital embedded in the ionization continuum. Shape resonant states are very short-lived and decay via tunneling to the single core-hole state, in the present case $(O\ 1s)^{-1}$, which further deexcite via normal Auger decay. The doubly charged normal Auger final states most likely dissociate into two singly charged fragments. The detection of both ions will result in too high intensity of the resonance D in the TIY as compared to the below-edge resonance C.
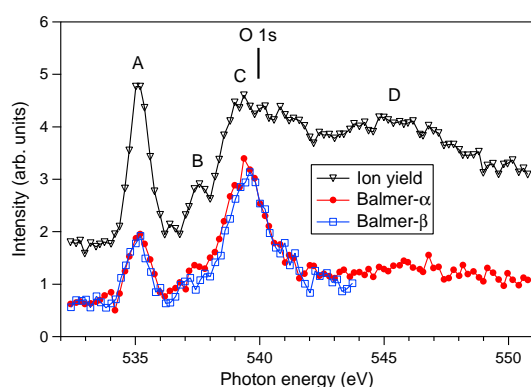
Figure 1. The total ion, Balmer-α and Balmer-β yields measured at the O 1s edge of the furan molecule. Photon energy resolution was about 0.4 eV.
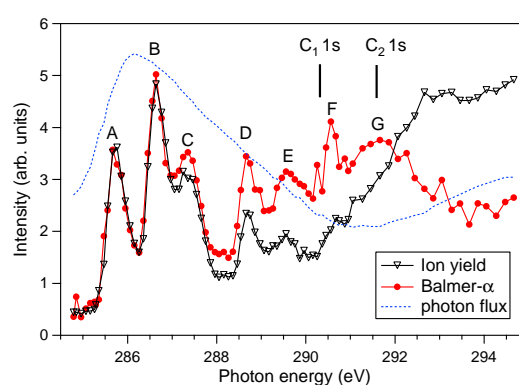
Figure 2. The total ion and Balmer-α yields measured at the C 1s edge of the furan molecule. Photon energy resolution was about 0.2 eV.

The resonances A-C are also visible in the Balmer-α yield (figure 1), but with different intensity ratios as in the TIY. The Balmer-α intensity is largest just before the O 1s IP. In the previous studies, such as the one of H_2O [5], the intensity increase in the region immediately below the core IP could easily be attributed to Rydberg excitations. The situation is more complicated in furan because the high-n Rydberg excitations can not be resolved from the molecular σ^* resonances just below the O 1s IP. It is likely that both molecular and Rydberg excitations contribute to the production of excited H atoms. The Balmer-β yield gives some evidence for the role of the Rydberg excitations. The relative intensities of the features in the Balmer-α and -β yields are almost the same, but the maximum just below the O 1s IP appears at $\sim$0.2 eV higher energy in the Balmer-β yield. That feature is also slightly narrower (by $\sim$0.2 eV) in the Balmer-β yield than in the Balmer-α yield. These observations can be explained if partly different Rydberg excitations lead to the production of the H atoms in the states n=3 and n=4. In contrast, it is less credible that different vibrations within the molecular σ^* resonances would invoke, after core hole decay, the dissociation of the molecule to the different quantum states of the H atom. We also observe that the Balmer-α yield displays a weak feature at energies of about 544–549 eV, but this feature does not exactly coincide with the σ^* (C-C) resonance (D) in the TIY. We tentatively attribute the weak structure to double excitations. Double excitations generally occur below shake-up photoionization thresholds, the lowest of which in O 1s photoionization of furan has been reported to be 6.7 eV above the O 1s IP of 539.95 eV [9].

The features A-G in the TIY at the C 1s edge of furan (figure 2) have already been observed before [8, 10]. The intensity ratios among the different resonances do not appear correctly in our measurement for the following reasons. Firstly, as discussed above, the TIY is affected by the increased ion production at photon energies above the inner shell IP. Secondly, the percentage

of higher order radiation from the beam line can vary as a function of photon energy due to the carbon contamination on the beamline optics, and the normalization to the photon flux, as has been done in the present work, may consequently change the intensity ratios. The photon flux as measured is shown in figure 2.

Based on calculations, Duflot *et al* [8] ascribed most intensity in the C 1s absorption spectrum to excitations to the molecular orbitals. The two empty π^* orbitals located in the bound part of the spectrum are mainly responsible for the resonances A-D. The excitations appear as two overlapping series because the carbon atoms have two different chemical environments. The corresponding IPs [10] are labelled as C_1 1s and C_2 1s in figure 2. The higher IP belongs to the carbon atom that is bonded to O. In the Balmer-α yield, the resonances A and B appear with the same intensity ratio as in the TIY, which is consistent with the core excitation taking place to the same π^* orbital. If the resonances C and D are compared, the relative intensity of the resonance D is higher in the Balmer-α yield. We ascribe this enhancement to the greater contribution of Rydberg excitations at the resonance D. The resonance E is due to the Rydberg excitations [8]. Accordingly, it is much enhanced in the Balmer-α yield. The resonance F is very weak in the TIY, but intense in the Balmer-α yield, and it is assigned to the Rydberg excitations that converge to the C_2 1s IP at 291.59 eV. The feature G in the Balmer-α yield just at the C_2 1s threshold is mostly due to the excitations to a σ^* orbital [8] whose maximum is at 291.8 eV. If it were due to core excitations to high Rydberg orbitals, a similar structure should appear at the C_1 1s threshold, which is not the case. In the TIY, the σ^* resonance (G) appears distorted with the maximum shifted above the threshold.

3.2. Carbon dioxide

Figure 3 displays a dispersed fluorescence spectrum in the wavelength region 820–855 nm measured at the O 1s $\rightarrow$ π^* excitation of CO_2. This region contains atomic emission lines from both neutral C and O [11]. The most intense line is due to the $2p^3(^4S)3p(^3P)$ - $2p^3(^4S)3s(^3S)$ transitions in neutral oxygen. Its excitation function is shown in figure 4 together with the TIY. The intensity scaling of the two curves is arbitrary, but clear differences can be seen in the relative intensities. In general, the oxygen emission is relatively more intense at all the Rydberg resonances than at the O 1s $\rightarrow$ π^* excitation. Furthermore, fluorescence becomes relatively stronger also on the high-energy side of the π^* resonance. We attribute this effect to the O 1s $\rightarrow$ 3s Rydberg excitation, whose presence as a high-energy shoulder of the π^* resonance is well known [12]. The Rydberg structure at $\sim$539.0 eV has been assigned to the vibrational structure of the O 1s $\rightarrow$ $3p\sigma$ and $4s\sigma$ excitations [13]. Here the excitation function of the oxygen emission line appears shifted to higher energies compared to the TIY, which may mean that the oxygen atom in this specific state is produced more efficiently when an vibrational excitation accompanies the electronic transition. Remarkably, the vibrational structures have been assigned to the antisymmetric stretching mode [13], the excitation of which may be imagined to favor the release of oxygen atoms. The proportional intensity increase of the oxygen emission line is highest at photon energies 540–540.5 eV, where excitations to higher Rydberg orbitals 4p, 5s, 5p and 6s are located [13]. The dispersed spectrum of figure 3 also shows the C emission line at 833 nm. Its intensity in the spectra measured at different photon energies was too low to draw any conclusions except that it resonates at the O 1s $\rightarrow$ π^* excitation.

It was shown for the core-excited water molecule that Lyman emission can follow when the core hole decays via spectator resonant Auger transitions [14]; the same conclusion is also valid for Balmer emission. If the core hole decayed through radiative channels, the final states would not have enough internal energy so that a bond could be broken and an excited H fragment released. A similar consideration of the decay channels can be done for CO_2. The resonant inelastic x-ray scattering (RIXS) spectrum (or soft x-ray emission spectrum) measured at the maximum of the O 1s $\rightarrow$ π^* excitation shows two peaks at the energies of $\sim$523 and $\sim$527 eV
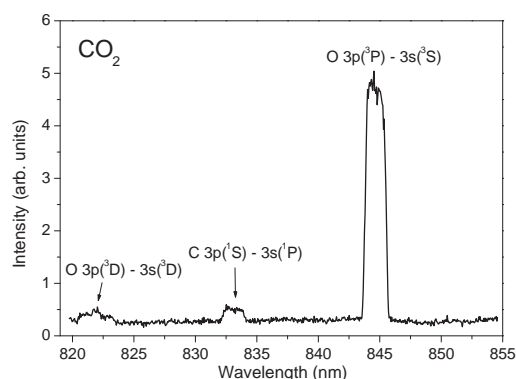
Figure 3. A dispersed fluorescence spectrum of CO_2 measured at the O 1s $\rightarrow$ π^* resonance. The occupation of the lowest electron shells in the labeled transitions is $1s^2 2s^2 2p^3$ for O and $1s^2 2s^2 2p^1$ for C.
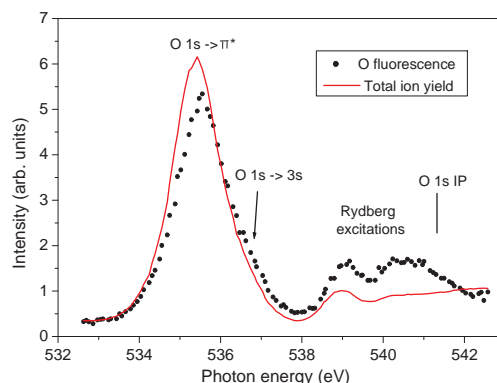
Figure 4. The excitation function of the O emission line at 845 nm (see figure 3) is shown with dots. The total ion yield measured simultaneously is shown with a solid line. Photon energy resolution was about 0.8 eV.

[15]. As the excitation energy at the resonance maximum is 535.4 eV, the binding energies of the RIXS final states are about 12.4 eV and 8.4 eV. The internal energy of the excited O atom, which fluoresces at 844.6 nm, is 10.99 eV [11], but the bond dissociation energy D(O=CO) of 5.451 eV is further required [16], setting the energy threshold at 16.44 eV. Therefore the observed fluorescence emission in the O atom at 844.6 nm can not follow the RIXS process. Resonant Auger decay leads to singly charged final states. The lowest dissociation energy for a channel that yields a neutral O atom and a charged fragment is 19.47 eV for $CO_2 \rightarrow CO^+ + O + e^-$ [16]. Thus, the final states of resonant Auger decay that have binding energies larger than 30.46 eV could dissociate so that an exited O fragment observed in our experiment is released. The experimental resonant Auger spectrum measured at the O 1s $\rightarrow$ π^* excitation reveals that a considerable part of the spectator final states are located at binding energies above 30.46 eV [17]. Hence fluorescence in O is energetically allowed after some spectator transitions from the O $1s^{-1}\pi^*$ state. The fraction of such final states increases at core-to-Rydberg excitations, as the relevant 2h-1p final states have the higher binding energies, the higher is the Rydberg orbital that the excited electron occupies.

It could therefore be deduced on the energetic grounds that fluorescence emission occurs more likely at the O 1s $\rightarrow$ Rydberg excitations than at the O 1s $\rightarrow$ π^* excitation. But the nature of the virtual orbital also plays a role. If the initial excitation is to a valence orbital, the same orbital is most probably occupied also in the 2h-1p final state, whereas the decay of the core-to-Rydberg excited states leads to the final states with an electron in a Rydberg orbital. The wavefunction of the diffuse Rydberg electron has less overlap with the molecular ion core than that of the more compact valence electron. Consequently, the valence electron is more likely to relax during dissociation, thereby resulting in an ion and a neutral fragment in the ground state [18]. Two-hole one particle (2h-1p) Rydberg states were suggested to produce particularly efficiently excited H atoms after core-to-Rydberg excitations [5]. The same mechanism should also be valid for molecules that do not contain H atoms. Indeed, the excitation function of the $2p^3(^4S)3p(^3P)$ state of oxygen (figure 4) provides evidence for this scenario: the highest relative intensity increase occurs in the region of Rydberg excitations. In CO_2, dissociation following resonant Auger decay may produce numerous excited states of neutral oxygen (and

carbon). The resulting fluorescence emission in neutral fragments is therefore distributed to many emission lines, instead of being concentrated in few peaks as in the Lyman or Balmer series in small hydrogen containing molecules such as water. Thus it is experimentally more challenging to determine the excitation functions of individual emission lines of oxygen atoms than those of hydrogen.

4. Conclusions

Fluorescence emission due to excited hydrogen and oxygen atoms has been measured at the core excitations of the furan and CO_2 molecules, respectively. In furan, there seems to be no site specificity due to the fact that the hydrogen atoms are bonded to the carbon atoms only: Balmer-α emission was found to increase at all core excitations below the O 1s and C 1s IPs. Core excitations to the valence and Rydberg orbitals overlap in furan, but fluorescence appears to take place more probably after core-to-Rydberg excitations. In CO_2, we followed the intensity behavior of a neutral oxygen emission line at $\sim$845 nm across the O 1s excitations. The emission was found to increase more at the O 1s $\rightarrow$ Rydberg excitations than at the O 1s $\rightarrow \pi^*$ excitation. Energetic considerations indicate that the emission in the O atom follows spectator decay of the core-excited states. Dissociation of the resulting 2h-1p states leads to excited fragments, and more often so when the excited electron is on a Rydberg orbital. This mechanism is supported by our measurements on CO_2 and furan.

Acknowledgments

References

[1] Kivimäki A, Vall-llosera G, Coreno M, Huels M A, Stankiewicz M and Rachlew E 2009 *J. Phys.* B **42** 075102
[2] Marquette A, Gisselbrecht M, Benten W and Meyer M 2000 *Phys. Rev.* A **62** 022513
[3] Chen J M, Lu K T, Lee J M, Ma C I and Lee Y Y 2004 *Phys. Rev. Lett.* **92** 243002
[4] Meyer M, Aloise S and Grum-Grzhimailo A 2002 *Phys. Rev. Lett.* **88** 223001
[5] Melero García E, Kivimäki A, Pettersson L G M, Álvarez Ruiz J, Coreno M, de Simone M, Richter R and Prince K C 2006 *Phys. Rev. Lett.* **96** 063003
[6] Kivimäki A, de Simone M, Coreno M, Melero García E, Álvarez Ruiz J, Richter R and Prince K C 2007 *Phys. Rev.* A **75** 014503
[7] Prince K C et al 1998 *J. Synch. Rad.* **5** 565
[8] Duflot A, Flament J-P, Giuliani A, Heinesch J and Hubin-Franskin M-J 2003 *J. Chem. Phys.* **119** 8946
[9] Chambers S A and Thomas T D 1977 *J. Chem. Phys.* **67** 2596
[10] Rennie E E, Hergenhahn U, Kugeler O, Rüdel A, Marburger S and Bradshaw A M 2002 *J. Chem. Phys.* **117** 6524
[11] Ralchenko Yu, Kramida A E, Reader J and NIST ASD Team 2008 *NIST Atomic Spectra Database (version 3.1.5)*, available at http://physics.nist.gov/asd3
[12] Piancastelli M N, Kivimäki A, Kempgens B, Neeb M, Maier K and Bradshaw A M 1997 *Chem. Phys. Lett.* **274** 13
[13] Okada K, Yoshida H, Senba Y, Kamimori K, Tamenori Y, Ohashi H, Ueda K and Ibuki T 2002 *Phys. Rev.* A **66** 032503
[14] Kivimäki A, Coreno M, Richter R, Álvarez Ruiz J, Melero García E, de Simone M, Feyer V, Vall-llosera G and Prince K C 2006 *J. Phys.* B **39** 1101
[15] Skytt P, Glans P, Guo J-H, Gunnelin K, Såthe C, Nordgren J, Gel'mukhanov F Kh, Cesar A and Ågren H 1996 *Phys. Rev. Lett.* **77** 5037
[16] Locht R and Davister M 1995 *Int. J. Mass Spectrosc.* **144** 105
[17] Carroll T X and Thomas T D 1991 *J. Chem. Phys.* **94** 11
[18] Rosenberg R A, Wen C-R, Tan K and Chen J-M 1990 *J. Chem. Phys.* **92** 5196